LARGE-SCALE CONTROLLED SURFACE EXPLOSIONS AT SAYARIM, ISRAEL, AT DIFFERENT WEATHER PATTERNS, FOR INFRASOUND CALIBRATION OF THE INTERNATIONAL MONITORING SYSTEM

Yefim Gitterman[1], Jeffrey Given[2], John Coyne[2], Roger Waxler[3],
Jessie Bonner[4], Lassina Zerbo[2], and Rami Hofstetter[1]

Geophysical Institute of Israel[1], CTBTO[2], University of Mississippi[3], and Weston Geophysical Corp.[4]

Sponsored by the Army Space and Missile Defense Command and Defense Threat Reduction Agency

Award Nos. W9113M-07-C-0189[1,3] and FA8718-09-C-0051[4]

ABSTRACT

Two large-scale calibration shots of 10 tons and 100 tons of ANFO explosives were successfully conducted by the Geophysical Institute of Israel (GII) at the Sayarim Military Range, Negev desert, Israel, on 24 and 26 January 2011, at different times of day. The explosives were assembled as a pyramid/hemisphere on the soft sediment surface, and detonated upward. Near-source high-pressures in air-shock waves were measured, and agreed with expected values for these charges.

The experiment was a collaborative effort between the CTBTO in Vienna, Israel, Middle East, European countries, and the USA, with the main goal to provide fully controlled ground truth (GT0) infrasound sources, monitored by extensive observations for calibration of International Monitoring System (IMS) infrasound stations in Europe, Middle East and Asia. The 2011 calibration experiment was intended to contribute to the understanding of the infrasound propagation in the atmosphere under winter conditions and improve IMS monitoring capabilities.

Institutions from more than 20 countries collaborated to set up a dense infrasound network for the period of the explosions. High-pressure gauges were deployed between 100 and 600 meters of the explosion to verify the designed yields of the explosions. Seismo-acoustic-overpressure stations were deployed at near-source distances (2-37 km) to capture the partitioning of seismo-acoustic energy. These data show that local wind conditions, measured by radiosonde just prior to the 100 ton explosion enhance overpressure amplitudes south of the explosion beyond 5 km. Portable infrasound arrays (20) were deployed in 13 countries throughout the Eastern-Mediterranean region in order to provide high-quality records for local-to-regional distances. The signals from the 100 tons explosion were observed at IMS infrasound stations in Russia, Kazakhstan, and Mongolia up to a distance of 6,250 km.

GII conducted a previous calibration explosion of a similar yield at the same Sayarim site in August 2009 under summer weather conditions (i.e. different stratospheric wind directions), and clear infrasound signals were recorded at many regional and IMS stations to the west and north-west, up to a distance 3,500 km, near Paris, France.

This pair of large-scale explosions (the strongest since the establishment of the IMS network) in different seasons demonstrated clear favorable westward and eastward propagation as predicted by the weather patterns. An extensive dataset of audio-visual, acoustic, seismic and infrasound records was collected from 0.1-6,250 km through a broad international collaboration.

OBJECTIVES

- Provide fully controlled strong infrasound sources, monitored extensively for calibration of IMS infrasound stations in Europe, Middle East and Asia;
- Contribute to the understanding of infrasound propagation and its seasonal (summer and winter) variation, and
- Calibrate the detection capability of the IMS infrasound network in the Eastern Mediterranean region.

RESEARCH ACCOMPLISHED

Two large-scale surface calibration explosions were successfully conducted by the GII at the Sayarim Military Range, Negev desert, Israel, on 24 and 26 January 2011. The experiment was a joint initiative of GII and the CTBTO, Vienna, and it was performed in close cooperation with the United States, European and Middle East countries. This “Winter” experiment was complementary to the previous “Summer” explosion of a similar size conducted by GII on 26 August 2009, supported by the U.S. Army SMDC (Gitterman, 2010).

Charge design. The experiment included two on-surface explosions of 10 tons and 102 tons of explosives, conducted in different times of day. The details of charge design are important for understanding of observed explosion effects and energy generation. The explosives were assembled as a pyramid/hemisphere on the soft sediment surface and detonated upward. The primary agent for these explosions was an ANFO mixture (94% Ammonium Nitrate and 6.0-6.1% Fuel Oil) placed in big bag waterproof packages (870 kg of ANFO in each). The velocity of detonation 2400 m/s and density 0.80-0.81 g/cm^3 were measured by the supplier in several tests. Mines M-15 provided by the Israel Defense Forces (IDF) were used in the charge boosters (each one 10 kg of HE explosive Composition B).

Design schemes for the charges, boosters and initiation system were provided by the IDF team according to concepts elaborated by GII. The design was intended to produce maximal energy release to the atmosphere (Figure 1): 1) an approximately hemispherical, compact shape with several layers of big bags without sharp corners in the layers; 2) a strong booster of mines M-15 placed inside and beneath a plastic box in the center of the ground layer providing the upward detonation direction; 3) a multiple-initiation scheme to provide an additional upward cumulative effect using 6 mines placed upside down on the ground beneath the plastic box and attached to detonators; 4) minimal air voids between charge layers (by removal of wooden platforms); 5) single mines beneath each bag (double mines for the upper layer) for reinforcement of the detonation wave front propagating upward; and 6) 38 additional mines placed in air-voids in 4 corners of the 1st layer (9-10 in each corner).

a b

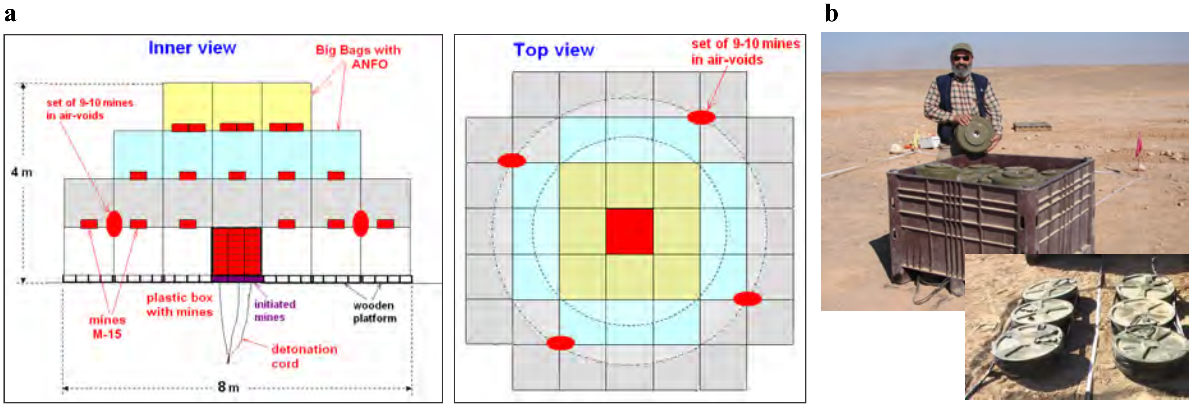

Figure 1. Design scheme and initiation system for the 102 ton charge (a); the booster view: six mines converted upside-down beneath the box with 84 mines M-15, placed at the site center (b).

In total the 102 ton charge was composed of 115 big bags of ANFO (870 kg in each bag, total 100,000 kg ANFO) and 208 mines M-15: 90 in the booster and 118 between the layers and in air voids at the corners (Figure 1a) – for a total nominal weight of 102,080 kg (Figure 2a). The small charge consisted of 9 big bags and 3 plastic boxes with bulk ANFO from 2.5 bags (580 kg in each box, total 10,000 kg ANFO) and 24 mines M-15 (240 kg Composition B) – for a total nominal weight 10,240 kg (Figure 2b).

The distance between the two explosions was 655 m (Figure 2b). The distance between the 102-ton charge and the previous 82-ton explosion (Summer 2009) was about 30 m (Figure 3).

a **b**

Figure 2. View of the main 102 ton charge assembled of four layers of big bags, with measured dimensions: base 8 Î 8 m, height 4 m (a), and the small charge 10 tons, remote by distance 655 m (b).

Conducting of the Explosions and GT0 parameters. Per IDF safety requirements, the territory within 6 km of the large explosion was surveyed by helicopter about 2 hours before the detonation to ensure that no people or animals were in the area (Figure 3).

GII organized on-line video broadcasting for both explosions using the digital network cameras used to monitor security (see the layout map on Figure 4). The real time picture was displayed on monitors at the Command Post, PTS CTBTO office in Vienna, and at GII.

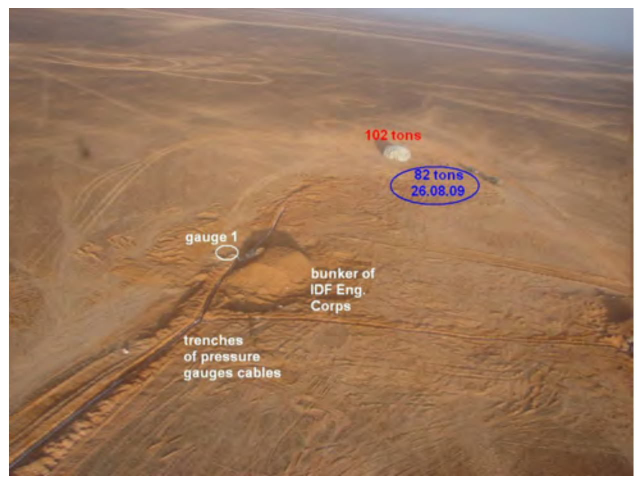

Figure 3. Helicopter view of the large explosion site. The place of the previous 82-ton explosion conducted by GII is shown, when distance between the charge centers is about 30 m.

Table 1 shows the Origin (detonation) Time (OT), GPS coordinates (accuracy 4-5 m) and local seismic magnitude M_d of the explosions. The OT values were based on an electric wire circle attached to the detonator with appropriate PC-based system with GPS time and finalized after analysis of raw data files from the GII data acquisition system and verification by accelerometer records. Explosion Ex1 was conducted as late as possible in the afternoon given the short daytime in January and Ex2 was conducted as early as possible in the morning. The duration magnitude, M_d, was estimated by Israel Seismic Network (ISN). Approximately 2 hours before Ex2, a small test, Ex3 (one M-15 mine), was conducted near the instrumentation bunker to check/tune the high-pressure measurement system and the speed video-camera.

Table 1. GT0 parameters of the explosions.

Event	Nominal charge weight (kg)	Date	Origin Time (GMT)	Local Seismic magnitude (M_d)	Latitude	Longitude	Elevation (m)
Ex1	10,240	01/24/2011	13:17:53.80	2.2	29.99555	34.81668	546
Ex2	102,080	01/26/2011	7:17:42.44	2.8	30.00064	34.81324	558
Ex3	10	01/26/2011	4:59:05.640	-	29.99901	34.81309	~554

Near-source observations. GII deployed different measuring and observation systems close distances including pressure gauges, accelerometers and video-cameras. The experiment layout of the explosion and recording systems is shown on Figure 4a. The maximal height of the dust and gases column was estimated using recordings of a video-camera: ~1250 m for Ex1 (after ~4 min), and ~2750 m for Ex2 (after ~6 min) (Rafael company, personal communication). The cloud from the 102 ton explosion was seen from over 37 km away.

a **b** **c**

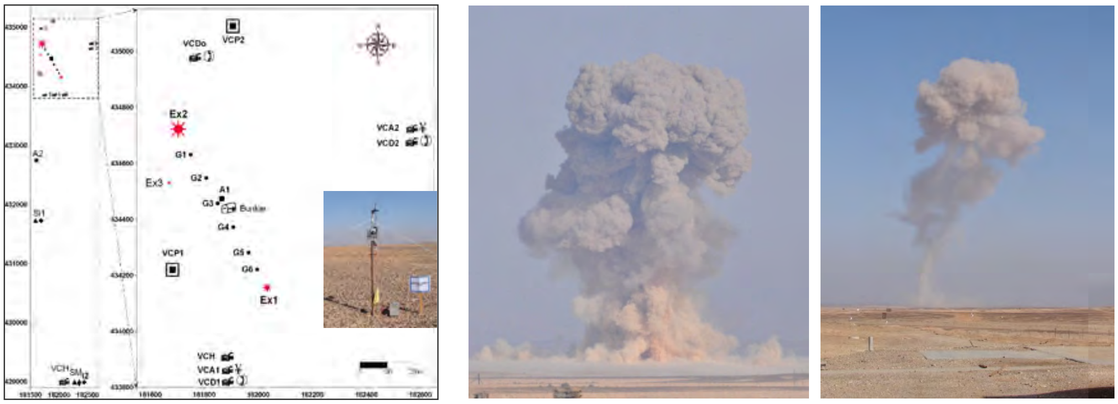

Figure 4. Experiment layout: location of explosions and near-source measurement systems, installed by GII: pressure gauges (G1-G6), accelerometers (A1,A2), home and speed video-cameras, and monitoring safety cameras that were broadcasting the real time video through internet (a); view of the dust and gases column from the Command Post at 6 km for Ex2 at 7.5 sec after detonation (b), and at 6 min (c).

High-pressure measurements. The high-pressure sensors were required to evaluate the efficiency of the charge design and energy generation of ANFO explosives and estimate the energy released by the explosions. Furthermore, the records of air-shock waves were used to analyze and explain some interesting blast phenomena. The IDF team installed six pressure gauges XTL-190-5G/50A/100A in a line (the GII profile) in the distance range 100-600 m (Figure 4a). The gauges with disc type baffles were mounted on steel rods ~1.5 m above the surface providing side-on free-field over-pressure measurements with sampling rate 2 MHz. Samples of the air-shock overpressure records are presented on Figure 5, together with calculated wave impulse (blue curves).

a **b** **c**

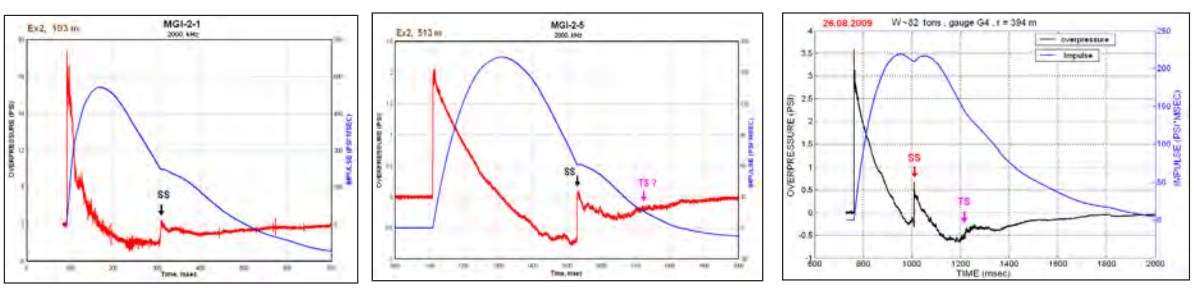

Figure 5. Samples of records at GII profile gauges for Ex1 (a) and Ex2 (b) at different distances. Gauge G5 for Ex2 showed SS delay ~0.42 sec, compared to a smaller ~0.24 sec delay, for the previous explosion (26.08.09), at a similar distance (c). Tertiary shocks (TS) are supposedly identified at some gauges.

For all gauges, a distinct secondary shock (SS) wave was observed during the negative phase of the pressure-time curves, showing negative or close to zero peak pressures. It is similar to SS waves observed for surface 20 and 100 ton ANFO shots in Alberta, Canada (Swisdak and Sadwin, 1970), and opposite to the case of the 2009 explosion conducted by GII, where positive SS peak pressures were observed (Figure 5c). The 2009 explosion comprised cast IMI explosives with higher density and velocity of detonation than the ANFO used in 2011 (Gitterman, 2010).

Evidently these strong explosives caused smaller time delays between main and secondary shocks resulting in positive SS peak pressures (Figure 5).

In this known, but rarely reported phenomenon, the blast wave for any finite explosion source can exhibit numerous repeated shocks (secondary and tertiary) of small amplitudes at various times, caused by successive implosion of rarefaction waves from the contact surface between explosion products and air (Baker, 1973). A higher pressure shock front propagates faster, therefore the time delay between the main shock (MS) and SS phases increases with distance. A preliminary estimate shows a nearly linear relationship between the delay and the logarithmic distance (Figure 6).

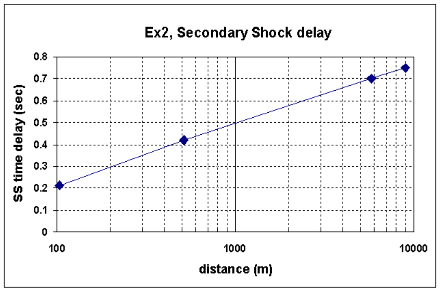

Figure 6. Time delay between MS and SS phases vs. log-scale distance for Ex2.

Accelerometers records. Two Kinematrics K2 accelerometers (A1 and A2 in Figure 4a) were placed on the surface and subjected to the impact of the strong air shock wave. For the 102 ton shot Ex2, a vertical acceleration up to 4g was measured at the closest station (Figure 7), corresponding to the main air-shock; weaker secondary shocks were also observed. Origin Time values for Ex1&2 were verified based on seismic arrivals of *P*-waves to accelerometers, and an available shallow subsurface velocity model at Sayarim Valley (Gitterman et al., 2005).

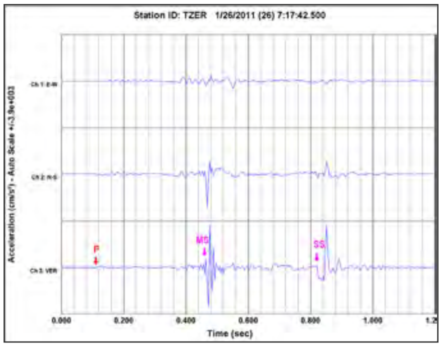

Figure 7. Accelerogram of Ex2 at A1 (~300 m), shown arrivals for P-waves, and main (MS) and secondary air-shocks (SS).

Audio-visual observations of blast effects. Two home video-cameras, three special safety monitoring cameras (radio and cellular transmitted), and a speed Phantom-3 (3000 frames/sec) camera were placed at different distances and azimuths for the two explosions (Figure 4) and recorded some interesting unique blast phenomena. Snapshots from home video of the 102-ton shot show an expanding short-term white (vaporization) spherical cap, clearly visible due to specific air (humidity 61%, temperature 13ºC) and lighting conditions. Snapshots of speed video-record for 10 ton shot show non-spherical segments and multiple phases in the air-shock wave front at short times and distances (Figure 8). Apparently, the same multiple shock-front phases were also observed in the large Ex2 and correspond to multiple peaks in the positive (compression) phase of the air-shock wave recorded by close pressure gauges (Figure 5a). Evidently, these front phases/peaks are due to the non-uniform charges, and cannot be attributed to any specific charge elements. Away from the explosion, the peaks are merged, and after ~70-100 m, a stable uniform shock wave is formed.

Many observers at the observation point at ~9 km from Ex2 reported hearing two clear "booms" with a delay less than 1 sec and interpreted them as two separate explosions. Multiple clear "booms" were also pronounced at recordings of monitoring video-cameras (at several hundreds meters) for both shots Ex1 and Ex2. This effect initially suggested that these calibration shots were not simultaneous as planned.

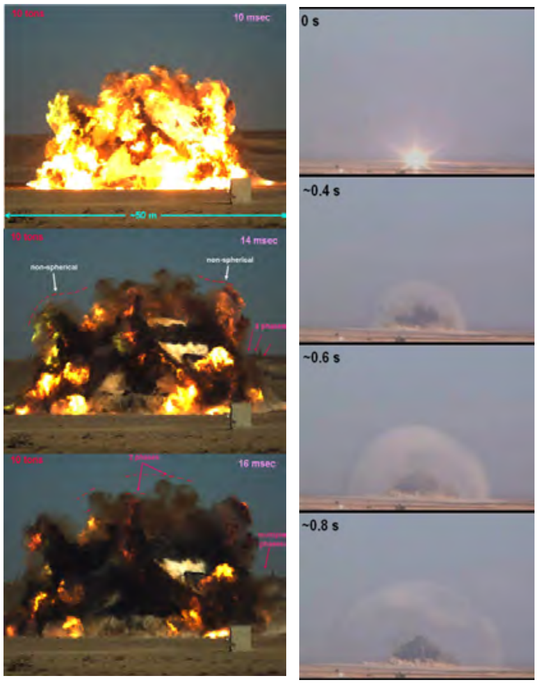

Figure 8. Snapshots from speed video-recording for Ex1 at 360 m (left) and from usual video recording at 6 km for Ex2 (right), show unique blast effects.

However, analysis of recorded data showed that these audio-phenomena were caused by secondary shocks in the air-blast wave observed at all records of high-pressure gauges and accelerometers (Figures 5,7). These observations, along with the yield estimates using the main-shock peak pressures confirm that all explosive materials were fully detonated in the initial 2-3 ms (see Table 2).

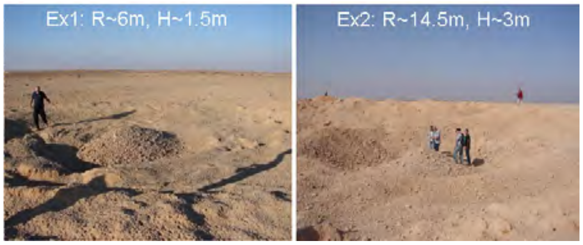

Figure 9. Crater general view for Ex1 and Ex2.

Crater observations. A complex irregular-shaped crater was found for both shots, with step-like walls and a cone of crashed rocks in the center (Figure 9). The shapes were different from the previous 82 ton explosion in 2009 with a regular hemispherical crater (radius 13.5 m, depth 5 m) (Gitterman, 2010). The crater was smaller than expected for this surface charge confirming a decreased coupling of explosive energy to the ground due to the specific charge design and especially the upward detonation.

Meteorological Observations. A radiosonde was launched by GII at the Command Post (Figure 10), approximately 1 hour before the detonation of Ex2, to provide atmospheric parameters (temperature, wind direction and velocity) at altitudes up to 25 km, for infrasound propagation modeling and interpretation of obtained observations (presented in following sections).

Figure 10. Launching the radiosonde and tracing by a radio-theodolite.

Estimation of TNT equivalent Yield. Estimations of TNT equivalent yield are based on BECv4 procedure, an Excel template (Swisdak M., 2000), taking into account actual altitude and air temperature. We utilized (with small corrections) peak pressure and maximal (positive phase) impulse values at GII profile gauges (only 3 gauges for Ex1), estimated by the IDF team (Table 2). The gauge G1 was excluded from the yield estimation for Ex2 due to anomalously low (for this distance 103 m) pressure amplitudes, supposedly because the shock propagation had not yet stabilized and may have been affected by the nearby IDF bunker (see Figure 4).

Table 2. Peak Pressure and Impulse at GII profile gauges and estimation TNT equivalent for Ex1 (altitude 546 m, T=24°C) and Ex2 (altitude 558 m, T=13°C).

Event	Gauge	Distance (m)	Peak over-pressure		Positive phase Impulse	
			measured (psi)	TNT yield (ton)	measured (psi*msec)	TNT yield (ton)
Ex1	G1	552	0.61	10.2	30.2	7.5
	G2	452	~0.80	10.5	36.6	7.4
	G3	351	~1.05	9.5	48.1	7.7
				average 10.07		**average 7.53**
Ex2	G2	203	~8	112	351	72
	G3	303	~4.3	128	251	76
	G4	405	~2.7	120	191	76
	G5	513	~2	130	165	86
	G6	580	1.6	116	137	78
				average 121		**average 78**

Note that a ratio of estimations based on peak over-pressure and maximal impulse is 121/78 = 1.55 and it is similar to the estimations we obtained for the Summer 2009 Sayarim explosion: 152/96 = 1.58 (Gitterman, 2010). An expected value for Ex1 is 8.6 ton, and for Ex2 is 86 tons, based on the standard ANFO to TNT efficiency is ~0.83. The positive phase impulse is the integral and stable characteristic of the air-blast wave (unlike the one-point peak over-pressure amplitude) and we consider the impulse-based estimates to be the most reliable, the same as for the 2009 explosion. The obtained yield estimates are a little smaller than the expected values (~25% for Ex1, and ~10%

for Ex2). We note several possible factors of lower air-blast energy and appropriate reduced TNT yield: 1) not quite hemispherical shapes (especially for Ex1); 2) inhomogeneous charges (bags and boxes for Ex1, placement of numerous mines with much stronger explosives in the ANFO charge body for Ex2); 3) air-voids between the charge units (plastic boxes and big bags). All these factors caused a non-uniform charge that resulted in observed blast anomalies: jetting, asymmetrical blast fronts, multiple shock-wave phases, turbulence, collisions of wave fronts (see Figure 8), and consequently in some energy losses. Finally, the accepted TNT equivalent charges are: **Ex1: W = 7.5 tons; Ex2: W = 78 tons.**

Seismo-Acoustic Energy Partitioning at Local Distances. Defining the seismo-acoustic source function for shallow or surface explosions remains an important problem for the explosion monitoring community. A team of US scientists from Weston Geophysical Corporation (WGC) and the Defense Threat Reduction Agency (DTRA) deployed six seismo-acoustic stations within 1-6 km of ground zero (GZ) the Sayarim Ground Truth (GT) explosions. The stations included a 1 Hz Sercel L4-3C velocity seismometer and either a Validyne 0.5 or 0.125 PSI overpressure sensor. Figure 11 shows the WGC/DTRA seismo-acoustic network combined with IDF overpressure sensors at distances between 0.1 and 0.6 km, the University of Mississippi (UM) acoustic gauges at 5, 10, 20, and 40 km, and the ISN stations. The network provided an excellent dataset of three different shots (Table 1), in order to study seismo-acoustic energy partitioning at local (< 100 km) distances.

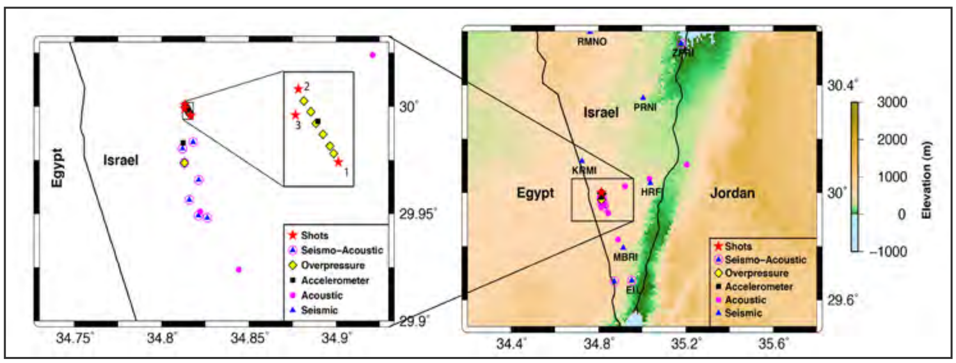

Figure 11. Near-source overpressure, seismic, and acoustic recordings of the Sayarim GT0 explosion series.

Figure 12 shows examples of the seismic data (at ~5km from GZ) and the overpressure data (at ~3 km from GZ). We completed particle motion analyses on the seismic data and identified *P*-waves, fundamental mode Rayleigh (*Rg*), and clear Love waves (SH) on the transverse components. We measured the peak particle velocity (PPV in cm/sec) at each station. For the overpressure data, we measured the maximum overpressure (in Pa) and the period between the impulsive start of the overpressure and its return to the equilibrium pressure. As expected, the periods and overpressures increase with increasing yield of the surface explosions. At a distance of 3 km and pressures below 100 Pa, the 10-kg Shot 3 has already lost the characteristic overpressure shape and appears oscillatory, indicating local propagation effects have possibly altered the signal characteristics for this explosion.

Figure 13 shows seismic PPVs and overpressures recorded from the 102-ton Shot 2 as a function of distance. Also shown are predicted PPVs based on a number of different published explosion-ground motion yield scaling relationships. These predicted PPVs were originally based on fully-confined explosions, but we have corrected them for a surface explosion using empirical data from the 2007 and 2009 HUMBLE REDWOOD (HR) explosions (Foxall et al., 2008, 2010). For the HR experiments, we observed factor of 2-3 reductions in amplitudes from fully-confined to surface/above-ground explosions. After the corrections, the Sayarim GT shots appear to fall between 1/X dry and wet alluvium models derived by Fuis et al. (2001) at distances < 10 km, while at greater distances there is substantially more scatter and the data cannot be constrained to a single ground motion scaling model. For future work, we will examine the scaling as a function of individual phases (e.g., *P*, *Rg*), instead of only considering the maximum PPV, in hopes of reducing the observed scatter.

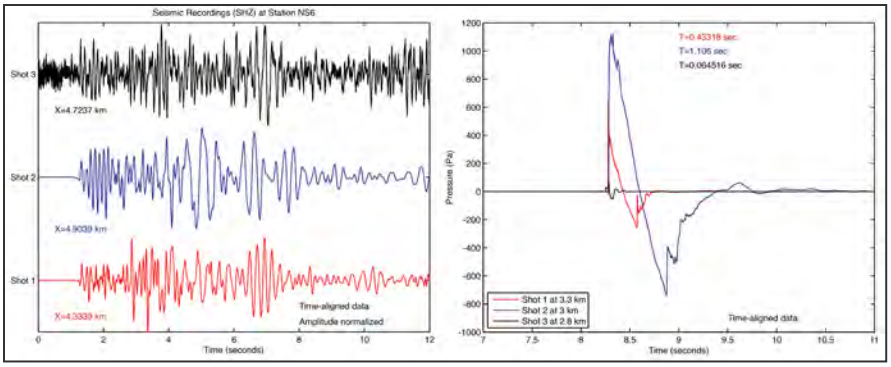

Figure 12. Seismograms (left) and overpressure signals (right) recorded from three Sayarim surface explosions. Note that Shot 2 (blue) is the 102-ton ANFO shot while Shot 3 was a mine detonated to test the blast initiation system.

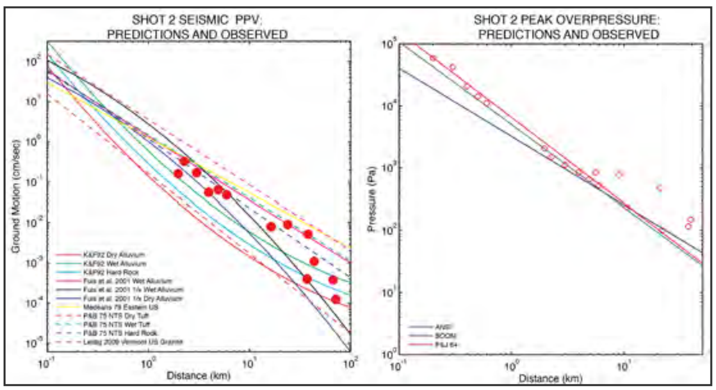

Figure 13. Observed PPV (left) and overpressures (right) from Shot 2 at distances up to 100 km and 40 km, respectively. Also shown are predictions using different ground motion scaling models and explosion overpressure models. The overpressure predictions are for a surface explosion, while the seismic predictions have been scaled from fully-confined to the surface.

Many of the overpressure amplitudes (Figure 13; right) from the 102-ton Shot 2 match closely to the predictions from the Perkins and Jackson (1964) and the BOOM (Lorentz, 1981) models. We note a bifurcation in the measured pressures at 5 km distance (or approximately 1000 Pa pressure). We observed that the overpressures that are above the predictions occur on stations south of GZ while stations east of GZ matched the predictions. Figure 14 suggests that local wind conditions were the cause of this bifurcation in the observed pressures from the 102-ton shot. A radiosonde deployed prior to Shot 2 (Figure 10) showed a low altitude S-SE wind flow peaked at about 1.8 km.

Modeling of acoustic propagation under such conditions (Figure 14; right) shows a distinct asymmetry in predicted acoustic amplitude. Due to this low altitude wind sound is ducted to the S-SE. This resulted in the pressure recordings to the south being as much as 4x larger than the recordings at similar distances to the east (Figure 14; left and middle). We note that a similar low altitude wind was not observed for the 10-ton Shot 1 on 24 January 2011, resulting in better agreements between the predicted and observed overpressure data from 0.1 to 40 km.

Regional and Long-range Infrasound Array Deployment and Signal Detection. Seasonal variability of long-range infrasound propagation is controlled primarily by the atmospheric winds. The most significant wind is the stratospheric jet, a zonal wind typically contained between the altitudes of 40 and 60 km. Also of significance is the jet stream, a tropospheric eastward flowing zonal wind typically concentrated at an altitude of 10 km. In Figure 15 below a time history of zonal wind amplitudes over the Negev Desert at 10 and 50 km altitude is shown. The atmospheric data was obtained from the U.S. Naval Research Lab (NRL) G2S model. Note that during the spring and summer the stratospheric jet is stable and flows consistently from east to west and the jet stream is weak. In the winter and fall the stratospheric jet is unstable, generally flowing from west to east, but with episodes, called sudden stratospheric warming events, during which its direction is uncertain. The jet stream is stable and strong during the winter and fall.

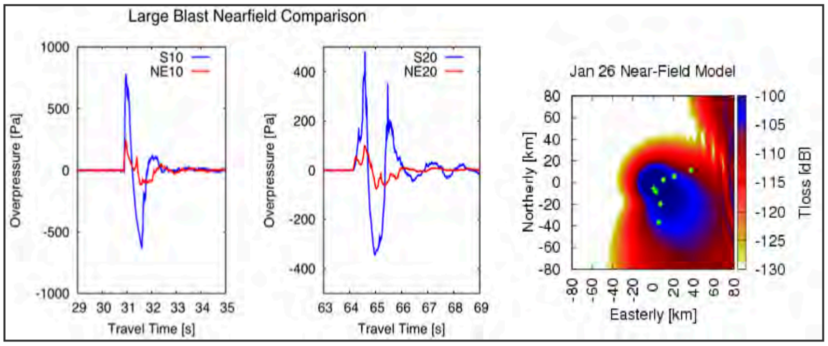

Figure 14. Observed pressures from UM sensors for the 102-ton shot at 10 and 20 km east (red) and south (blue) of GZ. At right is the acoustic propagation model based on wind conditions measured at GZ just prior to the shot. The model predicts favorable propagation conditions at local distances to the southeast of GZ.

To complement the 2009 summertime Sayarim experiment, a wintertime experiment was proposed. Under the US Nuclear Arms Control Technology (NACT) program, the National Center for Physical Acoustics (NCPA) of the UM worked with the CTBTO to plan and execute a large-scale deployment of infrasound arrays throughout the region. Although eastward propagation is more likely in the winter, making it necessary to pay particular attention to the regions east of Sayarim, given the unstable nature of the wintertime atmosphere, it was deemed necessary to instrument, to the extent possible, a full 360 degrees of azimuth about the Sayarim test site.

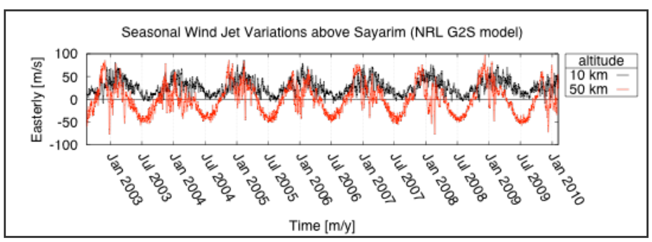

Figure 15. Seven year history of the most significant zonal winds above the Sayarim test range.

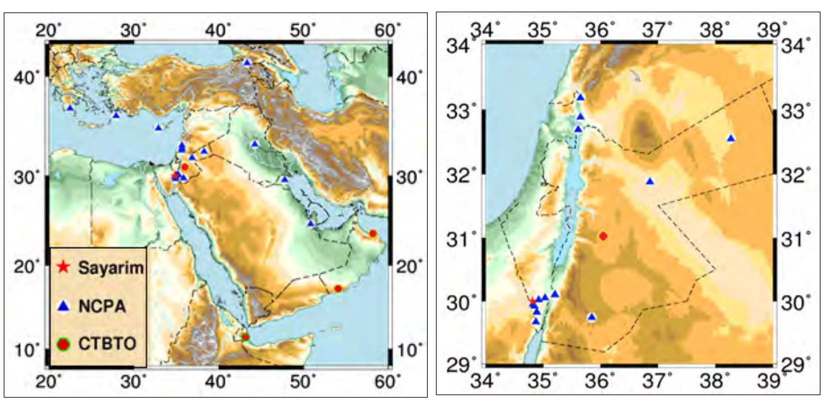

Figure 16. The locations of the temporary arrays deployed by NCPA and CTBTO. On the left is the entire deployment. On the right is a detail of the regional deployment in Israel and Jordan.

NCPA and CTBTO organized field teams of 23 researchers and technicians from the NCPA, CTBTO, U.S. Army Research Laboratory, University of Alaska Fairbanks and Qinetiq-North America to perform site surveys and then to deploy 21 temporary arrays with essential cooperation from local researchers. Arrays were deployed in Greece, Cyprus, Georgia, Kuwait, Iraq, Qatar, Oman, Djibouti, Jordan, and Israel, all with assistance from local geophysical institutes. In Figure 16, the locations of the temporary arrays deployed by the NCPA-CTBTO collaboration are shown. With the exception of the arrays in northern Israel, which had 5 and 6 elements, all the arrays were 4-element arrays with baseline from 700 to 1000 meters. The NCPA arrays used the NCPA digital infrasound microphones. The CTBTO arrays used the MB2005 microbarometers. Temporary arrays were also deployed in France by the French CEA, in Italy by the Geophysical Institute of Florence, and in Armenia by the Russian Ohbukhov Institute for Atmospheric Physics bringing the total number of far field temporary arrays to 20. In addition to the temporary arrays there are permanent infrasound arrays in Israel, Romania, Germany, France and the Netherlands as well as the CTBTO IMS infrasound network.

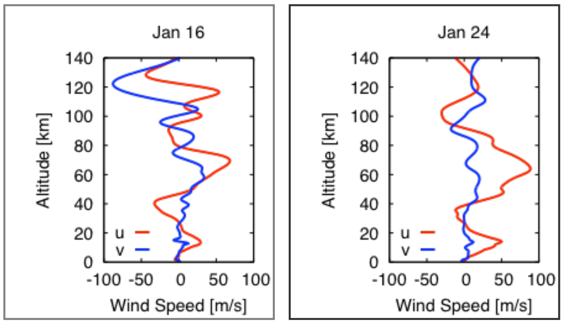

During the weeks prior to the calibration explosions the atmosphere was undergoing a sudden stratospheric warming event. However, by the weekend prior to the experiment the atmosphere had settled and a strong eastward flowing stratospheric jet had developed. In Figure 17, the NRL G2S profiles over Sayarim for 16 and 24 January 2011 are shown.

Figure 17. Zonal (u), and meridional (v) wind profiles over Sayarim from January 16 and 24, 2011 as given by the NRL G2S model.

Note that the 16 January profiles show a weaker jet stream and stratospheric winds flowing west at about 40 km, north at about 60 km, and east at about 70 km. The 24 January profiles show a stronger jet stream and predominantly eastward-flowing stratospheric winds. Had the experiment taken place during the week of 17 January 2011, rather than the week of 24 January, it is likely that signals would have been detected across Europe and the Middle East. As it was, for both the January 24 and January 26 shots no signals were detected at regional distances west of Sayarim while to the east signals were detected at great distances from the explosions. This is to be contrasted with the detections of the 28 August 2009 82-ton shot, which were all to the west.

In Figure 18, the locations of the detections made of the 26 August 2009, 82 ton shot are shown. In addition to the locations shown the GII deployed a line of microphones throughout Israel, all of which detected the shot. As expected for a summertime experiment there was strong westward propagation. While there is every reason to believe that there was no significant eastward propagation, there were no regional arrays deployed to the east to test the hypothesis. It can be said, however, that none of the IMS stations to the east detected the event.

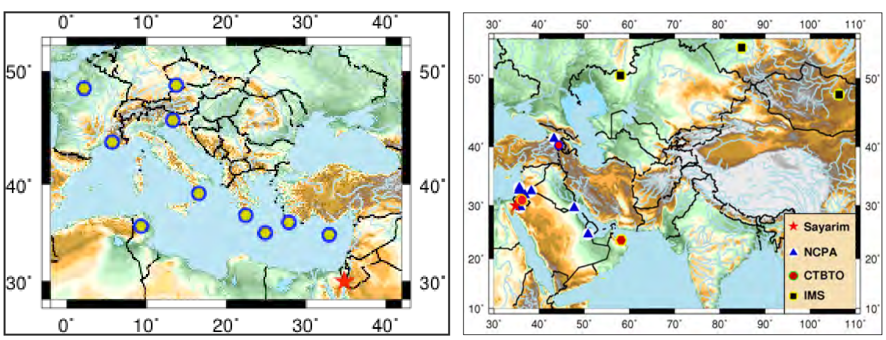

Figure 18. Map of known detections of the 82 ton shot on August 26, 2009 (left), and the 100 ton shot on January 26, 2011 (right).

In Figure 18, the locations of arrays that detected the 100 ton shot on 26 January 26 2011 are also shown. The signal was detected at three IMS stations: in Kazakstan, Russia and Mongolia. The Mongolia station is at 6250 km from Sayarim. There were logistical issues with the sensors deployed in Iraq, otherwise strong signals were detected at all of the arrays to the east with the sole exception of Djibouti, which is predominantly to the south. The received signals are currently being analyzed. Results of this analysis have, and will be, reported elsewhere.

CONCLUSIONS AND RECOMMENDATIONS

Two shots of about 100 tons yield, were successfully conducted by GII in Summer 2009 and Winter 2011. A pyramid/hemisphere charge design and the upward detonation direction enhanced explosion energy generation to the atmosphere for calibration of IMS infrasound arrays in Europe and Asia. The 2011 experiment was a collaboration between the CTBTO, Israel, the USA, and Middle East and European countries.

The main goal of this calibration experiment—to provide fully controlled infrasound sources (the strongest since the establishment of the IMS network) to be monitored by IMS infrasound stations in Europe, the Middle East and Asia—was reached. The infrasound signals were observed at numerous regional and IMS stations up to 3400 km to the west/north-west for the Summer Explosion in 2009, and up to 6250 km to the east for the Winter Explosion in 2011 - more than expected. The explosions established the first GT0 infrasound datasets for this region.

The complementary smaller Winter shot of 10 tons conducted during the afternoon two days before the main 102-ton explosion (conducted in the morning), provides additional valuable data for the analysis of charge scaling and infrasound propagation features affected by various atmospheric (wind) conditions. The unique database provides an important contribution in the modeling of infrasound propagation, detection analysis at different stations, and detectability issues of small surface nuclear tests.

ACKNOWLEDGEMENTS

Many organizations and persons participated in the preparation of the Winter 2011 calibration explosions, measurements and data processing. The Explosives Manufacturing Industries (1997), Israel (D. Hershkovich) supplied high-quality ANFO explosives in convenient package. The IDF Experiment Division (E. Stempler, Y. Hamshidyan) provided appropriate territory, logistics and near-source measurements, and assembled the charge with the optimal initiation/detonation scheme. The IDF Engineer Corps (Z. Savir) provided preparation of infrastructure for close-in measurements, and crater data processing. GII personnel helped in logistics procedures, prepared and installed numerous near-source observation systems and local infrasound stations and data processing (U. Peled, A. Shlomo, Y. Karmon, M. Kalmanovich, V. Giller, A. Shwarzburg, N. Perelman, V. Pinsky, T. Meirov, L. Feldman). Y. Ben-Horin (Israel NDC) provided assistance in promotion of the project and supplied good infrasound data.

Jessie Bonner wishes to thank DTRA for funding the WGC participation in the Sayarim experiment as well as Dr. Phillip Cole, Maj. Todd Ewy, Mr. Mark Leidig, and Dr. Aaron Ferris for deploying the sensors and recording the explosions. Extended thanks are to Mr. Leidig for his excellent logistic support throughout the planning stages of our involvement with the experiment, to Jim Lewkowicz for his unending drive and support for the WGC field program, to Dr. Robert Reinke, Al Leverette, Dr. Rodney Whitaker, and Dr. Stephen Arrowsmith for their support. Finally, the WGC/DTRA team thanks Dr. Y. Gitterman for allowing us to participate in the experiment, providing an excellent set of explosions to record, and not allowing us to wander too far into various dangers associated with an active bombing range.

Roger Waxler wishes to thank the U.S. Army Space and Missile Defense Command (SMDC) for funding the NCPA participation in the Sayarim experiment as well as the entire NCPA-CTBTO team. Particular thanks go to Eric Freimark and LaTonya Weekly for getting 87 sensors shipped to diverse locations in Europe and the Middle East in time to record this data.

CTBTO acknowledges Pierrick Mialle and Julien Marty for their relentless attention to details. Invaluable help came from the IMS engineering team that fabricated the hundreds of porous hoses necessary to deploy the sensors and the logistics team, in particular Reinhard Jelinek, that managed to ship 4 sensor arrays and all of the hoses at virtually the last minute. CTBTO also thanks CEA (France) and BGR (Germany) for providing equipment for two of the micro-barograph arrays.

REFERENCES

Baker, W. E. (1973). *Explosions in Air*, University of Texas Press, Austin and London, 268p.

Gitterman, Y. (2010). Sayarim Infrasound Calibration Explosion: near-source and local observations and yield estimation, in *Proceedings of the 2010 Monitoring Research Review: Ground-Based Nuclear Explosion Monitoring Technologies*, LA-UR-10-05578, Vol. II, pp. 708–719.

Gitterman, Y., V. Pinsky, A.-Q. Amrat, D. Jaser, O. Mayyas, K. Nakanishi, and R. Hofstetter (2005). Source features, scaling and location of calibration explosions in Israel and Jordan for CTBT monitoring, *Isr. J. Earth Sci*., 54: 199-217.

Foxall, B. R., R. Reinke, C. Snelson, D. Seastrand, R. Marrs, O.R. Walton, and A.L. Ramirez. (2008). The HUMBLE REDWOOD Seismic/acoustic coupling experiments, Abs. *Seismol. Res. Letts*., 79.

Foxall, B., R. Marrs, E. Lenox, R. Reinke, D. Seastrand, J. Bonner, K. Mayeda, and C. Snelson. (2010). The HUMBLE REDWOOD seismic/acoustic coupling experiments: Joint inversion for yield using seismic, acoustic, and crater data, Abs. *Seismol. Res. Letts*., 81: 315.

Fuis, G. S., J. M. Murphy, D. A. Okaya, R. W. Clayton, P. M. Davis, K. Thygesen, S. A. Baher, T. Ryberg, M. L. Benthien, G. Simila, J. T. Perron, A. K. Yong, L. Reusser, W. J. Lutter, G. Kaip, M. D. Fort, I. Asudeh, R. Sell, J. R. Vanschaack, E. E. Criley, R. Kaderabek, W. M. Kohler, and N. H. Magnuski. (2001). Report for borehole explosion data acquired in the 1999 Los Angeles Region Seismic Experiment (LARSE II), Southern California: Part I, Description of the survey, U.S. Geological Survey Open-File Report, 01-408.

Lorentz, R. (1981). Noise abatement investigation for the Bloodsworth Island Target Range: Description of the test program and New Long Range Airblast Overpressure Prediction Method, Technical report, Naval Surface Weapons Center, Silver Springs, MD

Perkins, B., and W. F. Jackson. (1964). Handbook for prediction of air blast focusing, BRL Report 1240.

Swisdak, M. and Sadwin, L. (1970). Blast Characteristics of 20 and 100 Ton Hemispherical AN/FO Charges. NOL Data Report, NOL TR 70-32, 17 Mar 1970.

Swisdak M. (2000). DDESB Blast Effects Computer, Version 4.0.